

^3He - ^3He Scattering in ^3He -HeII Mixtures at Low Temperatures

B. R. Joudeh

Applied Physics Department, Faculty of Science, Tafila Technical University

P. O. Box: 179, Tafila 66110 (Jordan)

Tel: 96-27-9901-1683 E-mail: bjoudeh@ttu.edu.jo

Received: December 27, 2010

Accepted: January 23, 2011

doi:10.5539/mas.v5n2p25

Abstract

The total and viscosity cross sections of ^3He - ^3He collisions in HeII are calculated. The basic achievement of the paper is the prediction of the Ramsauer-Townsend effect in this mixture. The RT minimum appears as a result of a balance between attractive short-range and repulsive zero-range interactions. In the low-energy limit the cross sections are dominated by S-wave scattering. In this limit, these cross sections are strongly modified by many-body effects. The influence of S-scattering decreases with increasing pressure and concentration because of the overall repulsion of medium effects. The effect of the P-wave scattering appears as a resonance-like behavior (peak structure) in the total cross section. This peak structure increases with pressure and concentration. For high energies, these cross sections are independent of pressure and concentration. This indicates that the high-energy behavior is dominated by the self-energy contribution; and the medium effects can be neglected.

Keywords: Total and viscosity cross sections, ^3He -HeII mixtures, Ramsauer-Townsend effect, Mean free path

1. Introduction

Superfluidity and dimerization of ^3He atoms in HeII are outstanding problems in low-temperature physics within both experimental (Ebner and Edwards, 1970; Edwards and Pettersen, 1992) and theoretical (Krotscheck and Saarela, 1993; Boronat et al., 1993) frameworks. There are no doubts among theorists that superfluidity of the ^3He component must exist at very low temperatures. Until now all experimental efforts to observe it have failed (Bashkin and Meyerovich, 1981; Boronat et al., 1993; Tuoriniemi et al., 2002; König and Pobell, 1994; König et al., 1994; Shirahama, and Pobell; 1994; Ishimoto et al., 1987; Owers-Bradley et al., 1983). The dimerization of the ^3He component leads to the effective “bosonization” of the impurity system. As a result of dimer formation, the Fermi-Bose liquid of ^3He -HeII is replaced with a quantum liquid that contains two Bose components, ^4He and $^3\text{He}_2$ (Bashkin and Wojdylo, 2000).

A renewed interest has risen in the calculation of cross sections of ^3He -HeII mixtures, due to their importance in the cooling down to the mK-range (Chaudhry and Brisson, 2009). These cross sections provide useful information about the interactions experienced by the colliding atoms. In this work, the ^3He - ^3He cross sections in ^3He -HeII mixtures will be calculated to explore the Ramsauer-Townsend (RT) effect and a phase transition in ^3He -HeII mixtures. RT is the phenomenon occurring in the collision between particles. In this case, the total cross section exhibits a deep minimum at a particular value of the relative energy (Joachain, 1983). This deep minimum usually occurs at low energy and arises because the most significant partial wave cross section contributing to the total cross section (S-wave cross section) becomes equal to zero. Therefore, the mobility is a maximum (Borghesani, 2001) or, equivalently, the mean free path of atoms in the system is correspondingly large. Bardeen, Baym and Pines (Bardeen et al., 1967) predicted the existence of a supermobility state – characterized by the ^3He atoms moving in the ^4He -background with an exceedingly long mean free path. Explanation of the RT effect in low-energy scattering was one of the first successful applications of wave mechanics to collision problems. RT effect appears in electronic systems and in molecular ^4He - ^4He (Kampe et al., 1973; Lim and Larsen, 1981; Joudeh et al., 2010) as well as ^3He - ^3He (Grace et al., 1976; Sandouqa et al., 2010). The problem of the bound state of two ^3He atoms in HeII has motivated us to obtain accurate results for the scattering of ^3He atoms at very low temperatures (Bashkin and Wojdylo, 2000; Bashkin and Meyerovich, 1981).

The starting point in computing the ^3He - ^3He cross sections in HeII is the determination of the relative phase shifts. This can be done by solving the Lippmann-Schwinger (LS) integral equation using a matrix-inversion technique (Bishop et al., 1977). The basic input is the Campbell effective interaction potential (Campbell, 1967). For calculating the Campbell potential, we have used the highly-acclaimed interatomic helium potential,

HFDHE2 (Aziz et al., 1979; Janzen, Aziz, 1995) which is generally regarded as the most reliable He-He potential. These mixtures have an additional degree of freedom, which is the ^3He concentration. This degree of freedom enables us to study the density effect on the scattering properties. The rest of the paper is organized as follows. The underlying theoretical framework is presented in Section 2. The results are summarized and discussed in Section 3. Finally, in Section 4, the paper closes with some concluding remarks.

2. Theoretical Framework

2.1 LS t -matrix

In this subsection we shall treat our formalism briefly. The Lippmann-Schwinger (LS) t -matrix after angular momentum decomposition may be written as (Bishop et al., 1977, Joudeh et al., 2010):

$$t_\ell(\vec{p}, \vec{p}'; s, \vec{P}) = u_\ell(|\vec{p} - \vec{p}'|) + (2\pi)^{-3} \int d\vec{k} u_\ell(|\vec{p} - \vec{k}|) g_0(k, s) t_\ell(\vec{k}, \vec{p}'; s, \vec{P}). \quad (1)$$

Here: \vec{p} and \vec{p}' are the relative incoming and outgoing momenta; the parameter s is the total energy of the interacting pair in the center-of-mass frame and is given by

$$s \equiv 2\mu_3^* \left(2P_0 - \frac{P^2}{m_3^*} \right); \quad (2)$$

P_0 is the total energy of the pair; P^2 is the energy carried by the center of mass. Throughout this work we use units such that $\hbar = 2m_3 = k_B = 1$, k_B being Boltzmann's constant. The operator $u \equiv (2\mu_3^* / \hbar^2) V \equiv (b/2) V$, where V is the Fourier transform of a static central two-body potential and μ_3^* is the effective reduced mass of the ^3He interacting pair: $\mu_3^* = (1/2) m_3^* = (b/2) m_3$. The conversion factor is $(\hbar^2 / 2m_3) = 8.0425 \text{ K} \cdot \text{\AA}^2$. Using our system of units, we have

$$s = bP_0 - P^2. \quad (3)$$

The number density of ^3He particles in ^3He -HeII mixtures ρ_3 is given by

$$\rho_3 = \frac{0.6022x}{\omega_4(1 + \alpha x)} \text{\AA}^{-3}, \quad (4)$$

where ω_4 is the volume of ^4He atom and x is the ^3He concentration.

The factor α is the volume differential coefficient, representing the difference between the volume occupied by a ^3He atom and that occupied by the heavier ^4He atom. Table 1 shows α , m_3^* and ω_4 at two different values of P_r and x .

The free two-body Green's function $g_0(s)$ is defined as

$$g_0(\vec{k}, s) \equiv \frac{1}{k^2 - s - i\eta}. \quad (5)$$

The system of interacting real particles is described in terms of weakly-interacting quasiparticles; this justifies the use of free Green's functions. The quantity η is a positive infinitesimal in the scattering region and zero otherwise.

The Fourier-Bessel transform of the interatomic potential was calculated using a program originally constructed by Ghassib and coworkers for interhelium potentials (Bishop et al., 1977). We have used the effective interaction in configuration space between two ^3He quasiparticles embedded in HeII which is the sum of three physical effects (Campbell, 1967). The first is the direct ^3He - ^3He interaction, $V_{33}(r)$. To this end, the so-called HFDHE2 (Aziz et al., 1979; Janzen, Aziz, 1995) has been used. The second effect is the interaction between the ^3He atoms and the HeII background, $V_{34}(r)$. The third effect is associated with the ^4He - ^4He interaction, $V_{44}(r)$. The total effective interatomic potential between two ^3He atoms is, therefore,

$$V_{\text{eff}}(r) = V_{33}(r) + V_{34}(r) + V_{44}(r). \quad (6)$$

The medium effects in $^3\text{He-HeII}$ mixture can be incorporated through two central quantities: an effective mass m^* , and an effective interaction $V_{\text{eff}}(r)$. In general, $m_3^* > m_3$; thus, we have more localization, and hence, less zero-point energy. At the same time, however, V_{eff} is generally less attractive than $V(r)$ (Ghassib, 1984).

To calculate the real and imaginary parts of the t-matrix, it is convenient to define a real K-matrix

$$K_\ell(p, p'; s, P) \equiv u_\ell(p, p') - \frac{1}{2\pi^2} \int_0^\infty dk \frac{k^2 u_\ell(p, k; s) K_\ell(k, p'; s) - s u_\ell(p, \kappa) K_\ell(\kappa, p'; s)}{k^2 - s}; \quad (7)$$

$$\kappa \equiv \sqrt{s}.$$

The relative phase shift $\delta_\ell(p)$ can now be obtained from the parameterization

$$K_\ell(p, p; p^2) = -\frac{4\pi}{p} \tan \delta_\ell(p). \quad (8)$$

2.2 Cross sections

Suppose a particle with wave vector \vec{k} and orbital angular momentum $\vec{\ell}$ is incident on another particle initially at rest. The probability for the first particle to cross, or to pass through, a unit area surrounding the stationary particle is called the differential cross section and is given by

$$\frac{d\sigma}{d\Omega}(\theta, \phi) = |f(\theta, \phi)|^2, \quad (9)$$

$f(\theta, \phi)$ being the scattering amplitude.

If the force causing the scattering is central, the differential cross section will be independent of ϕ .

The differential cross section for fermions with spin S is defined by (Lim and Larsen, 1981)

$$\frac{d\sigma}{d\Omega}(\theta) = \frac{1}{2} \left[\left(\frac{S+1}{2S+1} \right) |f(\theta) - f(\pi - \theta)|^2 + \left(\frac{S}{2S+1} \right) |f(\theta) + f(\pi - \theta)|^2 \right]. \quad (10)$$

Here $f(\theta)$ is defined by (Landau, 1996) as

$$f(\theta) = \frac{1}{2ik} \sum_{\ell=0}^{\infty} (2\ell+1) [\exp(2i\delta_\ell(k; P, \beta)) - 1] P_\ell(\cos \theta), \quad (11)$$

$P_\ell(\cos \theta)$ being the first-kind Legendre polynomial of order ℓ .

A general expression for the integral cross sections is

$$\sigma_n = 2\pi \int_0^\pi (1 - \cos^n \theta) \frac{d\sigma}{d\Omega}(\theta) \sin \theta d\theta, \quad (12)$$

where $n = 1$ corresponds to the diffusion cross section σ_D ; θ is the center-of-mass scattering angle.

Substituting $n = 1$ in Eq. (12), we have

$$\sigma_D = 2\pi \int_0^\pi (1 - \cos \theta) \frac{d\sigma}{d\Omega}(\theta) \sin \theta d\theta. \quad (13)$$

In arriving at Eq. (13), we have used the fact that the first integral is even; whereas the second is odd and therefore vanishes:

$$\begin{aligned} \sigma_D &= 2\pi \int_0^\pi \frac{d\sigma}{d\Omega}(\theta) \sin \theta d\theta = \sigma_T \\ \sigma_D &= \frac{8\pi}{k^2} \left[\left(\frac{S+1}{2S+1} \right) \sum_{\ell(\text{odd})}^{\infty} (2\ell+1) \sin^2(\delta_\ell(k)) + \left(\frac{S}{2S+1} \right) \sum_{\ell(\text{even})}^{\infty} (2\ell+1) \sin^2(\delta_\ell(k)) \right]. \end{aligned} \quad (14)$$

The viscosity cross section σ_η is obtained by substituting $n = 2$ in Eq. (12):

$$\sigma_{\eta} = \frac{4\pi}{k^2} \left[\begin{aligned} & \left(\frac{S+1}{2S+1} \right) \sum_{\ell(\text{odd})}^{\infty} \frac{(\ell+1)(\ell+2)}{\left(\ell + \frac{3}{2} \right)} \sin^2(\delta_{\ell+2}(k) - \delta_{\ell}(k)) \\ & + \left(\frac{S}{2S+1} \right) \sum_{\ell(\text{even})}^{\infty} \frac{(\ell+1)(\ell+2)}{\left(\ell + \frac{3}{2} \right)} \sin^2(\delta_{\ell+2}(k) - \delta_{\ell}(k)) \end{aligned} \right]. \quad (15)$$

For ${}^3\text{He}$, $S = \frac{1}{2}$, and Eqs. (14) and (15) become

$$\sigma_T = \frac{6\pi}{k^2} \sum_{\ell(\text{odd})}^{\infty} (2\ell+1) \sin^2(\delta_{\ell}(k)) + \frac{2\pi}{k^2} \sum_{\ell(\text{even})}^{\infty} (2\ell+1) \sin^2(\delta_{\ell}(k)); \quad (16)$$

$$\begin{aligned} \sigma_{\eta} &= \frac{3\pi}{2k^2} \sum_{\ell(\text{odd})}^{\infty} \frac{(\ell+1)(\ell+2)}{\left(\ell + \frac{3}{2} \right)} \sin^2(\delta_{\ell+2}(k) - \delta_{\ell}(k)) \\ &+ \frac{\pi}{k^2} \sum_{\ell(\text{even})}^{\infty} \frac{(\ell+1)(\ell+2)}{\left(\ell + \frac{3}{2} \right)} \sin^2(\delta_{\ell+2}(k) - \delta_{\ell}(k)). \end{aligned} \quad (17)$$

3. Results and Discussion

Our results are summarized in Figs. (1-10) and Tables. (1-3) for the HFDHE2 potential. The principal physical quantities here are the total (diffusion) and viscosity cross sections for ${}^3\text{He}$ - ${}^3\text{He}$ scattering in HeII. It was found necessary to include partial waves up to $\ell = 14$ so as to obtain results accurate to better than $\sim 0.5\%$. In our figures, the velocity (upper scale) represents the corresponding velocity v_1 [m/s] of a projectile atom

$$v_1 = \frac{\hbar k}{m_3} = \frac{420.86 k [\text{\AA}^{-1}]}{m_3} \quad \text{on a stationary target atom } (v_2=0) \text{ as a function of } k [\text{\AA}^{-1}].$$

Fig. (1) shows the behavior of the total cross section σ_T and the ℓ -wave cross section σ_{ℓ} ($\ell = 0-2$) for ${}^3\text{He}$ - ${}^3\text{He}$ scattering in HeII as functions of k at $x = 5\%$ for $P_r = 0$ and $P_r = 9.85 \text{ atm}$. For $k < 0.5 \text{ \AA}^{-1}$, the S-wave cross section is dominant. With increasing k , S-wave scattering tends to decrease; whereas the contribution of the higher angular-momentum waves to the scattering increases. For $k > 2 \text{ \AA}^{-1}$, the total cross section is nearly constant. Fig. (2) displays σ_T and σ_{ℓ} cross sections as functions of k as in Fig. (1), but for $P_r = 9.85 \text{ atm}$. From this figure, it is noted that the P-wave contribution to the total cross section increases with increasing pressure. The presence of a potential centrifugal barrier that arises from the orbital angular momentum $\ell = 1$ of the collision leads to the existence of quasi-bound states which manifest themselves as a resonance-like behavior.

Fig. (3) displays σ_T as functions of k at $x = 5\%$ for $P_r = 0$ and $P_r = 9.85 \text{ atm}$. It is noted that S-wave scattering, and hence the total cross section, decreases with increasing pressure in the zero-energy limit because the effective interaction becomes shallower with increasing pressure (Al-Sugheir et al., 2006).

Figs. (4) and (5) show σ_T as a function of k for $x = 1.3\%$ and $x = 5\%$ at $P_r = 0$ and $P_r = 9.85 \text{ atm}$, respectively. It is noted that the high-concentration total cross sections are less than the corresponding low-concentration cross sections as $k \rightarrow 0$ because of the overall repulsion of medium effects, thanks to the overall less attraction of the V_{eff} .

Figs. (6) and (7) show the S-wave cross section σ_0 and the P-wave cross section σ_1 , respectively, as a function of k for $x = 1.3\%$ and $x = 5\%$ at $P_r = 9.85 \text{ atm}$. At low concentration $\sigma_0(0)$ is greater than that of high concentration. On the other hand, at low concentration $\sigma_1(0)$ is less than that of high concentration. It has been predicted that dilute ${}^3\text{He}$ -HeII mixtures favour S-scattering at low concentration (Efremov et al., 2000). On the other hand, at high concentration the interaction tends to produce p-scattering, because at low (high) concentration the S- (P-) scattering is dominant (Østgaard and Bashkin, 1992; Sandouqa et al., 2010).

As shown in Figs. (3-7), in the low energy limit, the ${}^3\text{He}$ - ${}^3\text{He}$ cross section σ_T decreases with increasing pressure and concentration. The mean free path ℓ_3 of the ${}^3\text{He}$ impurities in HeII is inversely proportional to σ_T (Kerscher et al., 2001). i.e., ℓ_3 increases as expected by Bardeen, Baym and Pines (Bardeen et al., 1967) who predicted the existence of a supermobility state in ${}^3\text{He}$ -HeII mixtures.

From the previous figures, we observe an RT minimum and a peak structure (resonance-like behavior) in the total cross section. Our results for RT are summarized in Table 2. This table shows the velocity v [m/s], the relative energy E [K], and the total cross section σ_T [\AA^2] at which RT occurs. The cross section depends on the concentration and pressure. By increasing the pressure, the atoms become more localized. It follows that the velocity, at which the RT minimum occurs, decreases with increasing pressure. Further, σ_T has a peak at a particular velocity, as shown in Table 3. This peak clearly appears by increasing the pressure and also by increasing the concentration. Judging from previous experience, this peak may be interpreted as an indicator of superfluidity or a quasi-bound state (Alm et al., 1994; Bohm, 1994). For high k , these cross sections are independent of pressure and concentration. This is because the kinetic energy part is much larger than the interaction part; therefore the medium effects become negligible, i.e., one can define a *free-atom* cross section appropriate for the energy range where the cross section is a constant.

Fig. (8) exhibits the viscosity cross section σ_η as a function of k at $x = 5\%$ for $P_r = 0$ and $P_r = 9.85$ atm. σ_η has the same behavior as the total cross section, i.e., they have an RT minimum and a resonance-like behavior. It is found the high-pressure viscosity cross sections, for $k > 2 \text{\AA}^{-1}$, approach the corresponding low-pressure cross sections. Therefore, for $k > 2 \text{\AA}^{-1}$, there are no strong quantum effects manifesting themselves because of the relatively small scattering length for the ^3He - ^3He scattering in ^3He -HeII mixtures (Bishop et al., 1977).

Figs. (9) and (10) show σ_η as a function of k at $P_r = 0$ and $P_r = 9.85$ atm for 1.3% and $x = 5\%$ respectively. By comparing these figures to Fig. 8, it is noted that the effect of concentration is similar to that of pressure.

4. Conclusion

In this paper, the cross sections of ^3He - ^3He collisions in HeII are calculated, namely, the total and viscosity, using the HFDHE2 potential. The basic achievement of the paper is the prediction of the Ramsauer-Townsend effect in this mixture. The RT minimum appears as a result of a balance between attractive short-range and repulsive zero-range interactions. The physical observation is that, at a particular value of energy, the total scattering cross section is anomalously small. At this energy, therefore, ^3He atoms propagate through the HeII background as essentially unscattered particles. Other achievements are: (1) the prediction of a phase transition due to resonance-like behavior in the total cross section; and (2) studying the effect of the pressure and concentration on these cross sections.

In the low-energy limit, the cross sections are dominated by S-wave scattering. In this limit, these cross sections are strongly modified by many-body effects. The influence of S-scattering decreases with increasing pressure and concentration because of the overall repulsion of medium effects. When the relative momentum is in the 0.5\AA^{-1} range and higher, the contributions from the higher angular momentum (P-wave and above) scattering may become significant. The effect of the P-wave scattering appears as a resonance-like behavior on the total cross section. This peak structure increases with pressure and concentration. For high energies, these cross sections are independent of pressure and concentration. This indicates that the high-energy behavior is dominated by the self-energy contribution, and the medium effects can be neglected.

In conclusion, our calculations for cross sections show that these quantities are useful indicators of phase transitions in ^3He -HeII mixtures. The most prominent effects found are resonance-like behavior and the Ramsauer-Townsend effect in the cross sections at low temperatures in these mixtures.

References

- Alm, T., Röpke, G., and Schmidt, M. (1994). Critical enhancement of the in-medium nucleon-nucleon cross-section at low temperatures. *Physical Review C*, 50, pp. 31-37.
- Al-Sugheir, M.K., Ghassib, H.B. and Joudeh, B.R. (2006). Fermi pairing in dilute ^3He -HeII Mixtures. *International Journal of Modern Physics B*, 20, pp. 2491-2504.
- Aziz, R.A., Nain, V.P.S., Carley, J.S., Taylor, W.L., McConville, G.T. (1979). An accurate interatomic potential for helium *J. Chem. Phys.* 70, pp. 4330-4341.
- Bardeen, J., Baym, G., and Pines, D. (1967). Effective Interaction of ^3He in ^4He at Low Temperature. *Phys. Rev.* 196 pp. 207-220.
- Bashkin, E.P., and Wojdylo, J. (2000). Dimerization of ^3He in ^3He - ^4He dilute mixtures filling narrow channels. *Phys. Rev. B*, 62, pp. 6614- 6628.
- Bashkin, E.P., and Meyerovich, A.E. (1981). ^3He - ^3He quantum solutions. *Advances in Physics*, 30, pp. 1-92.
- Bishop, R.F., Ghassib, H.B., and Strayer, M.R. (1977). Low-energy He-He interactions with phenomenological potentials. *Journal of Low Temperature Physics*, 26, pp. 669-690.

- Borghesani, A.F. (2001). Electron mobility maximum in dense argon gas at low temperature. *Journal of Electrostatics*, 53, pp. 89-106.
- Boronat, J., Polls, A., and Fabrocini, A. (1993). Structure properties of the ^3He - ^4He mixture at $T=0\text{K}$. *Journal of Low Temperature Physics*, 91, pp. 275-297.
- Bohm, A. (1979). *Quantum Mechanics: Foundations and Applications* (Springer, N.Y., first edition 1979; third edition 1994).
- Campbell, L. J. (1967). Effective Coordinate-Space Potential Between ^3He atoms in Superfluid ^4He . *Phys. Rev. Lett.*, 19, pp. 156-159.
- Chaudhry, G., and Brisson, J.G. (2009). Thermodynamic Properties of Liquid ^3He - ^4He Mixtures Between 0.15 K and 1.8 K. *Journal of Low Temperature Physics* 155, pp. 235–289.
- Ebner, C., and Edwards, D.O. (1970). The Low-Temperature Thermodynamic Properties of Superfluid Solutions of ^3He in ^4He . *Physics Reports C2*, pp. 77-154.
- Edwards, D.O., and Pettersen, M. S. (1992). Lectures on the Properties of Liquid and Solid ^3He - ^4He Mixtures at Low Temperatures. *Journal of Low Temperature Physics*, 87, pp. 473-523.
- Efremov, D.V., Mar'enko, M.S., Baranov, M.A., and Kangan, M.Yu. (2000). Superfluid Transition Temperature in a Fermi Gas with Repulsion. Higher Orders Perturbation Theory Corrections. *JETP*, 90, pp. 861.
- Ghassib, H. B. (1984). On Dimers and Trimers in Some Helium Fluids. *Z. Phys. B- Condensed Matter*, 56, pp. 91-98.
- Grace, R.S., Pope, W.M., Johson, D.L., and Skofronick, J.G. (1976). Ramsauer-Townsend effect in the total cross section of ^4He - ^4He and ^3He - ^3He . *Phys. Rev. A*, 14, pp. 1006-1008.
- Hsu, W., and Pines, D. (1985). Effective Interactions in Dilute Mixtures of ^3He in ^4He . *J Statistical Phys.*, 38, pp. 273-312.
- Ishimoto, H., Fukuyama, H., Nishida, N., Miura, Y., Takano, Y., Fukuda, T., Tazaki, T., and Ogawa, S. (1987). New spin-wave modes in ^3He - ^4He solution. *Phys. Rev. Lett*, 59, pp. 904-907.
- Janzen, A.R., Aziz, R.A. (1995). Modern He-He potentials: Another look at binding energy, effective range theory, retardation, and Efimov states. *J. Chem. Phys.*, 103, pp. 9626- 9830.
- Joachain, C. J. (1983). *Quantum Collision Theory*. (North-Holland Publishing Company, 1983).
- Joudeh, B.R., Sandouqa, A.S., Ghassib, H.B., and Al-Sugheir, M.K. (2010). ^3He - ^3He and ^4He - ^4He Cross Sections in Matter at Low Temperature. *Journal of Low Temperature Physics*, 161, pp. 348-366.
- Kampe, W.A., Oates, D.E., Schrader, W., and Bennewitz, H.G. (1973). Observation of the Atomic Ramsauer-Townsend Effect in ^4He - ^4He Scattering. *Chem. Phys.Lett.*, 18, pp. 323-324.
- Kerscher, H., Niemetz, M., and Schoepe, W. (2001). Viscosity and Mean Free Path of Very Diluted Solutions of ^3He in ^4He . *Journal of Low Temperature Physics*, 124, 163-168.
- König, R., and Pobell, F. (1994). Fermi Liquid Behaviour of the Viscosity of ^3He - ^4He Mixtures. *Journal of Low Temperature Physics*, 79, pp. 287-310.
- König, R., Betat, A. and Pobell, F. (1994). Refrigeration and Thermometry of Liquid ^3He - ^4He Mixtures in the Ballistic Regime. *Journal of Low Temperature Physics*, 97, pp. 311-333.
- Krotscheck, E., and Saarela, M. (1993). Theory of ^3He - ^4He mixtures: energetics, structure, and stability. *Phys. Rep.*, 232, pp. 1-86.
- Landau, R. *Quantum Mechanics II* 2nd edn (Wiley, New York, 1996).
- Lim, T.K., and Larsen, S.Y. (1981). The Ramsauer-Townsend effect in molecular systems of electron-spin-polarized hydrogen and helium and their isotopes. *J. Chem. Phys.* 74, pp. 4997-4999.
- Owers-Bradley, J.R., Chocholacs, H., Mueller, R.M., Buchal, Ch., Kubota, M., and Pobell, F. (1983). Spin Waves in Liquid ^3He - ^4He Mixtures. *Phys. Rev. Lett.*, 51, pp. 2120-2123.
- Østgaard, E., and Bashkin, E. (1992). Superfluidity of ^3He in dilute ^3He - ^4He mixtures. *Physica. B*, 178, pp. 134-140.
- Polturak, E., and Rosenbaum, R. (1981). Specific Heat of 5% and 3% ^3He - ^4He Solutions Under Pressure. *J low Temp. Phys.*, 43, pp. 477-498.

Sandouqa, A.S., Ghassib, H.B., and Joudeh, B.R. (2010). A Ramsauer–Townsend effect in liquid ^3He . *Chem. Phys. Lett.*, 490, pp. 172-175.

Sandouqa, A. S., Joudeh, B. R., Al-Sugheir, M.K., and Ghassib, H. B. Weak ^3He Pairing in ^3He –HeII Mixtures. Submitted for publication.

Shirahama, K., and Pobell, F. (1994). Search for ^3He superfluidity and measurement of ^3He inertial effective mass in ^3He – ^4He mixture films. *Phys. B*, 194, pp. 863-864.

Tuoriniemi, J., Martikainen, J., Pentti, E., Sebedash, A., Boldarev, S., and Pickett, G. (2002). Towards Superfluidity of ^3He Diluted by ^4He . *J. Low Temp. Phys.*, 129, pp. 531-545.

Watson, G. E., Reppy, J. D., and Richrdson, R. C. (1969). Low-Temperature Density and Solubility of ^3He in ^4He under Pressure. *Phys. Rev.* 188, pp. 384-396.

Table 1. α , m_3^* and ω_4 at two different values of x and P_r

x	$P_r = 0$			$P_r = 9.85 \text{ atm}$		
	α	m_3^*/m_3	ω_4	α	$m_3^*/m_3^{(a)}$	ω_4
5%	0.284 ^(a)	2.45 ^(a)	45.79 ^(b)	0.203 ^(a)	2.74 ^(a)	41.66 ^(b)
1.3%	0.284 ^(a)	2.38 ^(a, c)	45.79 ^(b)	0.202 ^(a)	2.64 ^(a)	41.66 ^(b)

^(a) (Polturak and Rosenbaum, 1981), ^(b) (Watson et al., 1969), ^(c) (Hsu and Pines, 1985)

Table 2. The Ramsauer-Townsend velocity v [m/s], the relative energy E [K] and total cross section σ_T [\AA^2], for two values of concentration and pressure

x	$P_r = 0$			$P_r = 9.85 \text{ atm}$		
	v [m/s]	E [K]	σ_T [\AA^2]	v [m/s]	E [K]	σ_T [\AA^2]
5%	25.85	0.074	328.5	13.63	0.043	335.5
1.3%	29.4	0.093	309.3	24.0	0.069	312.4

Table 3. The peak velocity v [m/s], the relative energy E [K] and total cross section σ_T [\AA^2], for two values of concentration and pressure

x	$P_r = 0$			$P_r = 9.85 \text{ atm}$		
	v [m/s]	E [K]	σ_T [\AA^2]	v [m/s]	E [K]	σ_T [\AA^2]
5%	47.5	0.25	598.3	39.4	0.19	765.3
1.3%	48.9	0.26	500.8	44.1	0.23	590.5

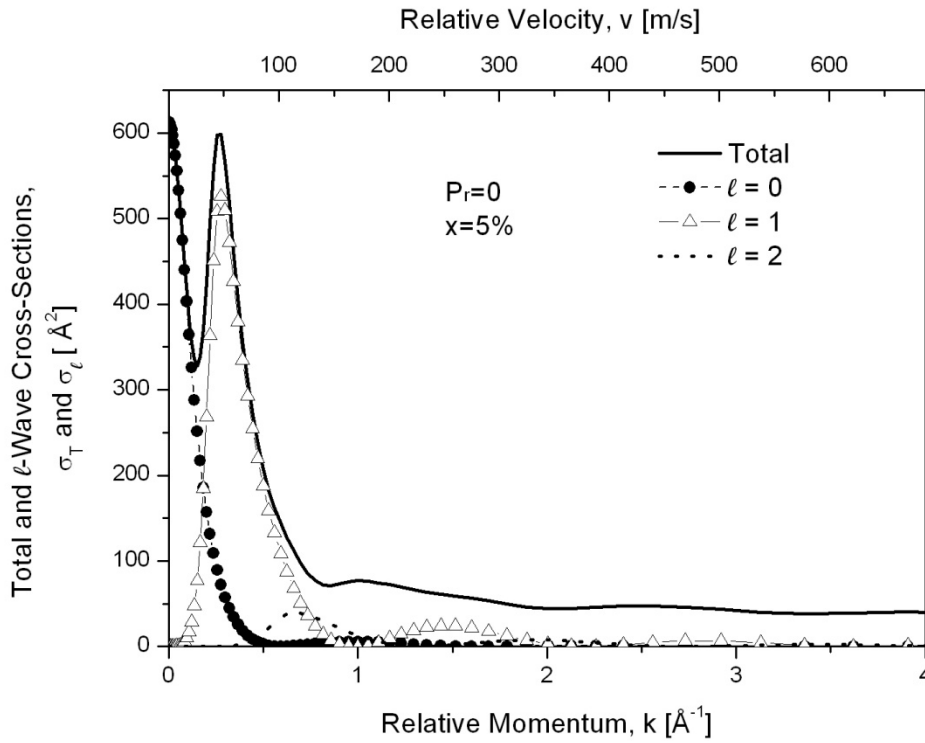


Figure 1. The total and ℓ -wave cross sections (σ_T and $\sigma_\ell [\text{\AA}^2]$) as functions of $k [\text{\AA}^{-1}]$ for concentration $x = 5\%$, $P_r = 0$. The upper scale [m/s] represents the corresponding velocity v of a projectile atom on a stationary target atom

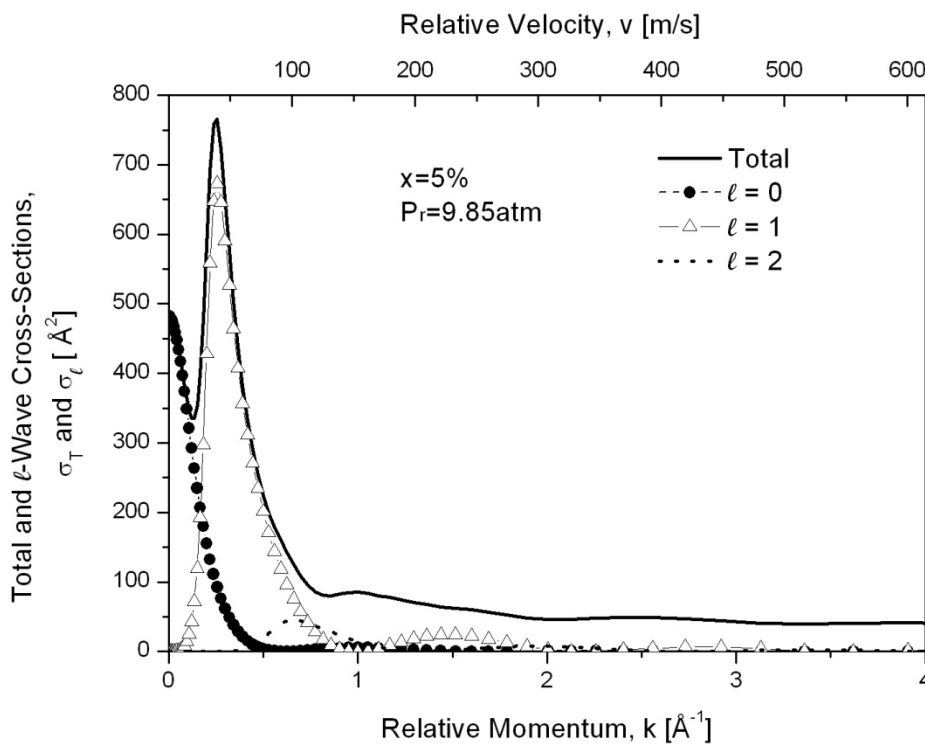


Figure 2. The same as in Fig. 1, but only for $P_r = 9.85 \text{ atm}$.

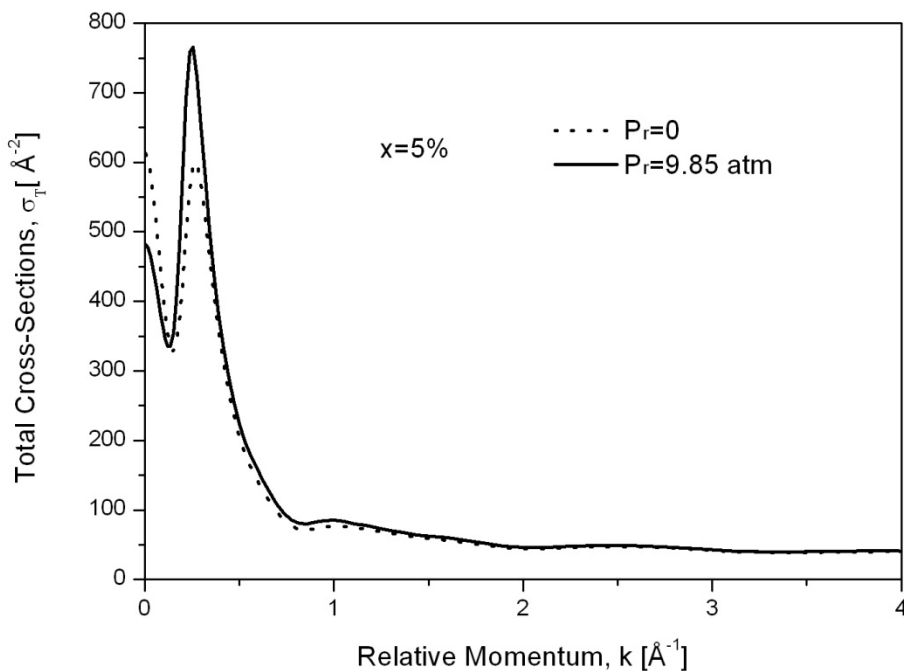


Figure 3. The total cross section $\sigma_T [\text{Å}^2]$ as a function of $k [\text{Å}^{-1}]$ at $x = 5\%$ and for two different values of pressure

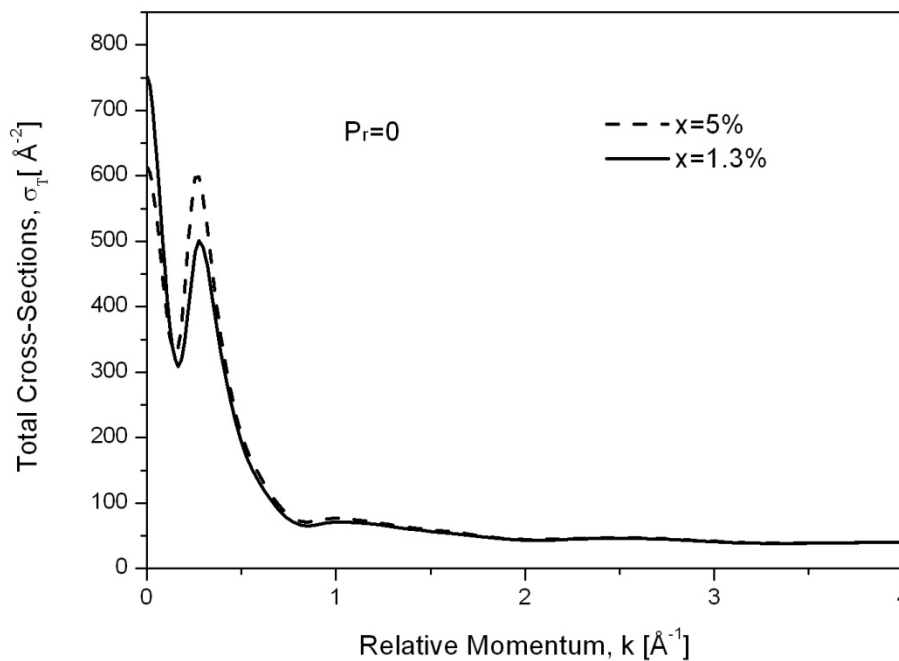


Figure 4. The total cross section $\sigma_T [\text{Å}^2]$ as a function of $k [\text{Å}^{-1}]$ for $P_r = 0$, and two different values of concentration

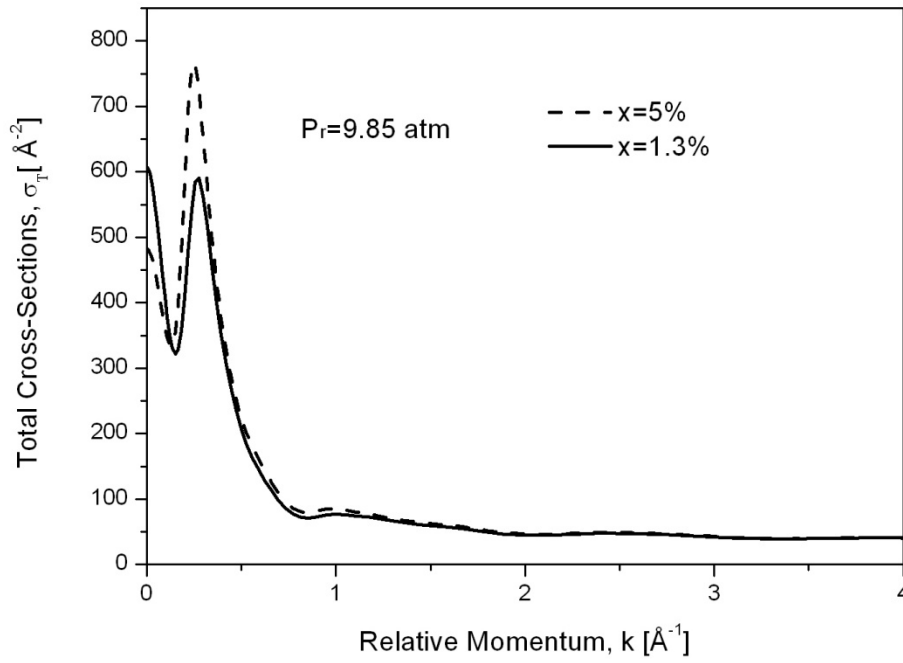


Figure 5. The same as in Fig. 4, but only for $P_r = 9.85 atm$.

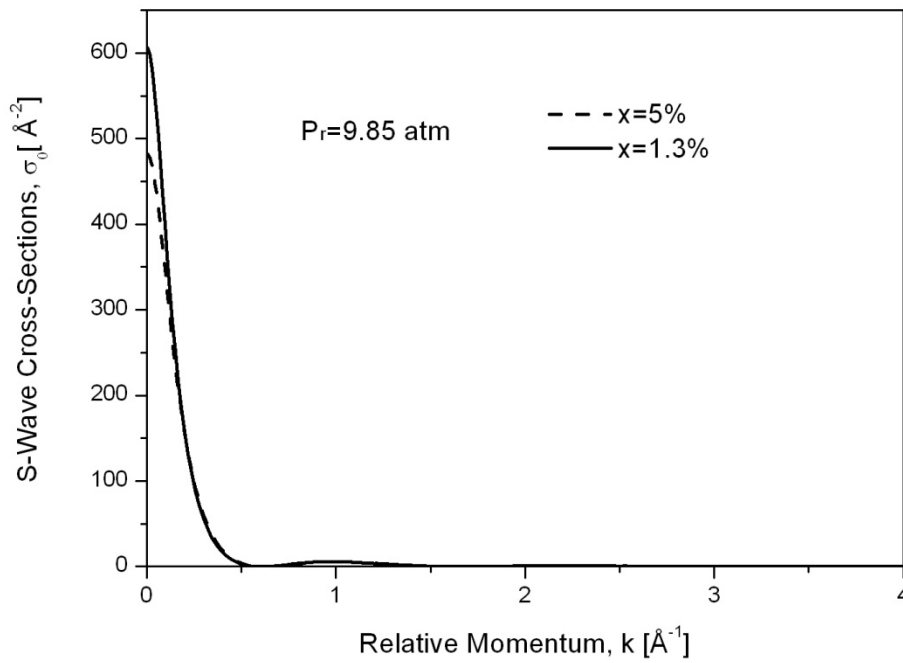


Figure 6. The S-wave cross section $\sigma_0 [A^2]$ as a function of $k [A^{-1}]$ for $P_r = 9.85 atm$, and two different values of concentration

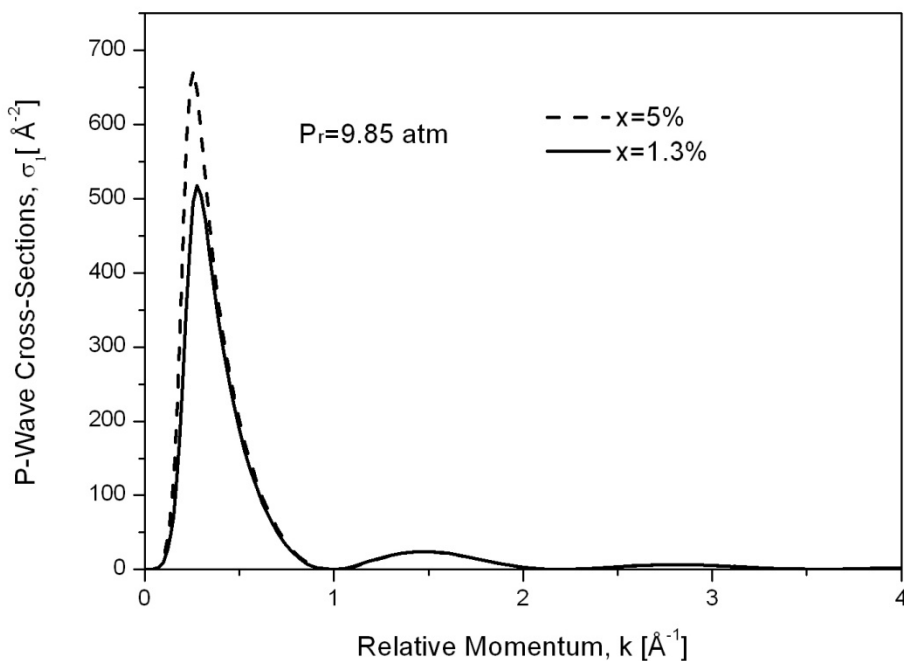


Figure 7. The same as in Fig. 6, but only for the P-wave cross section $\sigma_1 [A^2]$

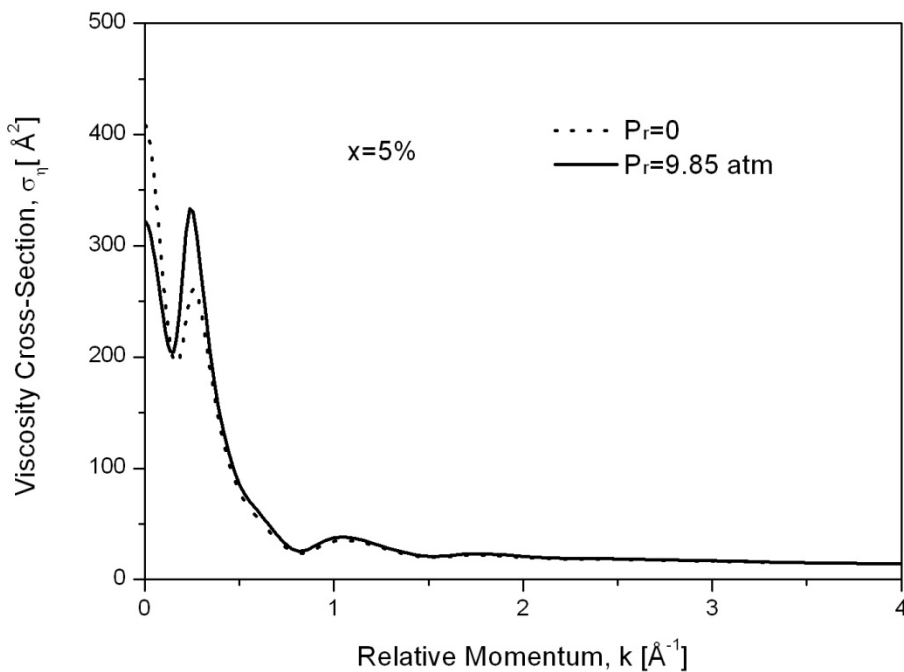


Figure 8. The viscosity cross section $\sigma_\eta [A^2]$ as a function of $k [A^{-1}]$, for $x = 5\%$ and for two different values of pressure

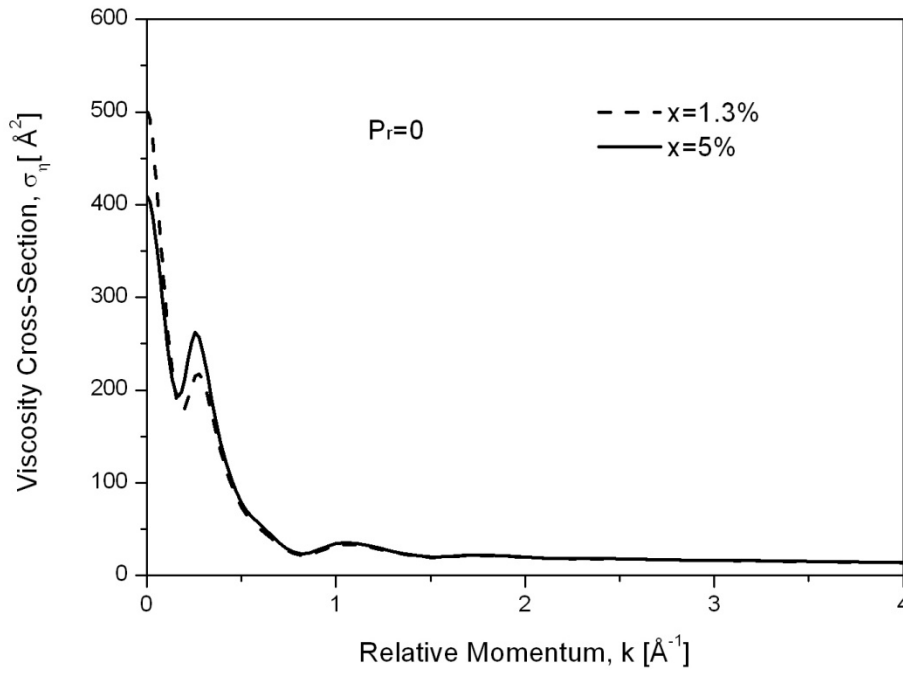


Figure 9. The viscosity cross section $\sigma_{\eta}[\text{\AA}^2]$ for $P_r = 0$, and two different values of concentration

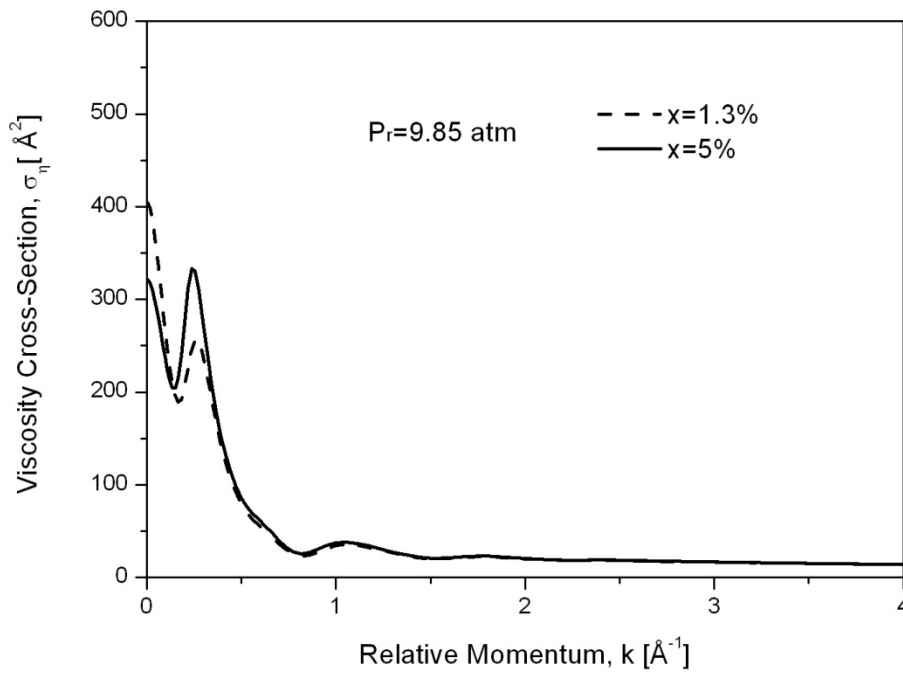


Figure 10. The same as in Fig. 9, but only for $P_r = 9.85 \text{ atm}$.